Discovery and Characterization of a 5-Hydroxymethylfurfural Oxidase from Methylovorus sp. Strain MP688

Dijkman, Willem P.; Fraaije, Marco W.

Published in:
Applied and environmental microbiology

DOI:
10.1128/AEM.03740-13

Publication date:
2014

AEM
Journals.ASM.org

Discovery and Characterization of a 5-Hydroxymethylfurfural Oxidase from *Methylovorus* sp. Strain MP688

Willem P. Dijkman, Marco W. Fraaije

Molecular Enzymology Group, Groningen Biomolecular Sciences and Biotechnology Institute, University of Groningen, Groningen, The Netherlands

In the search for useful and renewable chemical building blocks, 5-hydroxymethylfurfural (HMF) has emerged as a very promising candidate, as it can be prepared from sugars. HMF can be oxidized to 2,5-furandicarboxylic acid (FDCA), which is used as a substitute for petroleum-based terephthalate in polymer production. On the basis of a recently identified bacterial degradation pathway for HMF, candidate genes responsible for selective HMF oxidation have been identified. Heterologous expression of a protein from *Methylovorus* sp. strain MP688 in *Escherichia coli* and subsequent enzyme characterization showed that the respective gene indeed encodes an efficient HMF oxidase (HMFO). HMFO is a flavin adenine dinucleotide-containing oxidase and belongs to the glucose-methanol-choline-type flavoprotein oxidase family. Intriguingly, the activity of HMFO is not restricted to HMF, as it is active with a wide range of aromatic primary alcohols and aldehydes. The enzyme was shown to be relatively thermostable and active over a broad pH range. This makes HMFO a promising oxidative biocatalyst that can be used for the production of FDCA from HMF, a reaction involving both alcohol and aldehyde oxidations.

To switch from petroleum-based chemicals to biologically based and therefore renewable chemicals, new technologies and processes have to be developed (1). One promising biologically based chemical is 2,5-furandicarboxylic acid (FDCA). This chemical building block has been mentioned for many years as having great potential for future applications (1, 2). Recently, new technologies in the polymer industry have already led to the production of an FDCA-based polymer, polyethylene furanoate (PEF). This polyester displays characteristics similar to those of the well-known and widely applied compound polyethylene terephthalate but is based on FDCA instead of terephthalate. The application of FDCA is, however, not restricted to PEF and other polyesters, as it can be used in the preparation of polyamines and polyurethanes as well (2).

FDCA is a renewable compound, as it can be produced from fructose and other sugars. The production of FDCA starts from fructose and proceeds via the formation of 5-hydroxymethylfurfural (HMF) as an intermediate. In the first step, HMF is formed from fructose. This intramolecular dehydration step is acid catalyzed and takes place at relatively high temperatures (3). In the second part of the process, HMF is oxidized to FDCA (Fig. 1). The reaction that turns HMF into FDCA is a six-electron oxidation in which the alcohol group is oxidized to the corresponding aldehyde. This aldehyde group and the aldehyde group already present in HMF are further oxidized to the corresponding carboxylic acids, resulting in FDCA. The existing chemical methods for this reaction require the use of stoichiometric quantities of strong oxidants or involve metal salt catalysts in organic solvent and high temperature and pressure (4, 5). Thus, a gentler and less expensive enzymatic procedure is desirable.

Unlike chemical oxidation, enzymatic or whole-cell-catalyzed conversions can be performed at lower temperature and pressure. However, enzymes active on HMF are scarce. To date, only a few enzymes were shown to be active toward HMF (6, 7), of which only one oxidizes HMF, chloroperoxidase (CPO). CPO from *Caldariomyces fumago* is a heme-containing peroxidase producing mainly the single oxidized products diformyl furan (DFF) and 5-hydroxymethyl-2-furoic acid (HMF acid) (74 and 20%, respectively) from HMF. The triple-oxidation product FDCA is not formed (7).

Recently, HMF oxidase activity was identified in the bacterium *Cupriavidus basilensis* (8). This microbe harbors a gene cluster involved in HMF metabolism and is able to grow on HMF as a sole carbon source. One of the encoded genes is a putative oxidoreductase, HmfH, which presumably oxidizes HMF. The actual substrates used and the products formed by HmfH are, however, unclear. The HmfH-encoding gene has been introduced into a *Pseudomonas putida* strain that could subsequently be used in a fermentative process to produce FDCA from HMF. The *Pseudomonas* strain itself is able to produce HMF acid but not FDCA from HMF. Only when HmfH is expressed in *Pseudomonas* is FDCA formed (9). On the basis of these findings, it has been suggested that HmfH can perform both alcohol and aldehyde oxidations and therefore may be able to form FDCA from HMF. However, this has not yet been confirmed experimentally.

HmfH is a member of the glucose-methanol-choline (GMC) oxidoreductase protein family (10). Members of the GMC oxidoreductase family have two conserved domains. The N-terminal GMC domain (Pfam 00732) is involved in the binding of flavin adenine dinucleotide (FAD) as a prosthetic group. The FAD cofactor in GMC-type oxidases provides the oxidative power needed in the reactions and is reduced to $FADH^-$ upon oxidation of the substrate. The reduced cofactor is reoxidized by molecular oxygen, resulting in the formation of hydrogen peroxide along with the product. In some GMC flavoprotein oxidases, the FAD is covalently linked to a histidine side chain in this domain of the

Received 12 November 2013 **Accepted** 20 November 2013
Published ahead of print 22 November 2013
Address correspondence to Marco W. Fraaije, m.w.fraaije@rug.nl.
Supplemental material for this article may be found at http://dx.doi.org/10.1128/AEM.03740-13.

doi:10.1128/AEM.03740-13

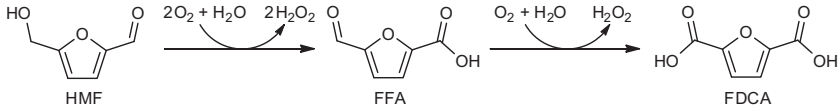

FIG 1 HMFO-catalyzed oxidation of HMF into FFA and FDCA. The reaction that turns HMF into FFA is a double oxidation that involves the transfer of four electrons from the substrates to the enzyme. In the reaction that turns FFA into FDCA, the aldehyde group is oxidized into the carboxylic acid.

enzyme. The second conserved domain is the C-terminal GMC domain (Pfam 05199). This roughly 150-amino-acid-long domain contains the active-site residues, including a strictly conserved histidine (11).

The substrates for GMC oxidoreductases are diverse, ranging from small alcohols like methanol and choline (12) to more complex compounds like glucose (13) and aromatic alcohols (14). While most GMC oxidases convert an alcohol to a ketone or an aldehyde, some are able to perform a double oxidation, converting a primary alcohol to the aldehyde and subsequently to the carboxylic acid. Overall, the substrate donates four electrons to the enzyme in such a reaction. However, only a few GMC oxidoreductases can oxidize alcohols to the corresponding carboxylic acids (12, 15). Although hydroxylations and amine oxidations have been described for other types of flavoprotein oxidases (16), thus far, no GMC flavoprotein oxidases with such activities have been identified (10).

In this paper, we describe the cloning of a gene from *Methylovorus* sp. strain MP688 that encodes an HmfH homologue. The corresponding enzyme could be overexpressed in *Escherichia coli* and purified by affinity chromatography. This enabled us to explore the biocatalytic properties of this enzyme, which turned out to be an effective FAD-containing oxidase that is able to oxidize HMF to FDCA. Therefore, we have named the enzyme HMFO (HMF oxidase). Intriguingly, the activity of HMFO is not restricted to HMF and many other aromatic substrates are efficiently oxidized as well.

MATERIALS AND METHODS

Expression, purification, and spectral analysis of HMFO. The genes encoding HMFO (YP_004038556.1), HmfH (ADE20408.1), and YP_001895804.1 from *Burkholderia phytofirmans* PsJN were purchased from DNA2.0 (Menlo Park, CA). The synthetic genes were optimized for expression in *E. coli*, and the HMFO- and *B. phytofirmans* PsJN-encoding genes included a sequence that encodes a C-terminal tobacco etch virus (TEV) protease cleavage site, followed by a Strep tag facilitating affinity chromatography purification (see Fig. S1 to S3 in the supplemental material). The genes were delivered in a pJexpress 404 plasmid from DNA2.0.

To increase expression levels, a SUMO-HMFO fusion construct was created. The *hmfo* gene was amplified from the pJexpress 404 plasmid with the following primers: forward, 5′-ATGACTGATACGATTTTTGACTACGTG-3′; reverse, 5′-TTAAGCCTGGGTCAGAATCGC-3′. The underlined bases introduce a stop codon behind the last residue of HMFO. This stop codon was introduced because it was not present in the ordered gene since it contained a C-terminal TEV protease site and a Strep tag for purification. The PCR product (2.9 μg) was incubated with 5 U of *Taq* polymerase and 0.6 mM dATP (both from New England BioLabs) in a total volume of 40 μl for 15 min at 72°C to introduce 3′-A overhangs. This DNA was ligated into the pET-SUMO vector as described in the Champion pET SUMO Protein Expression System user manual (Invitrogen, Carlsbad, CA).

For HMFO expression, an overnight culture of *E. coli* BL21(DE3) cells with the SUMO-HMFO coding plasmid was diluted 1:100 in 1 liter of Terrific Broth containing 50 $\mu g \cdot ml^{-1}$ kanamycin and grown at 37°C until it reached an optical density at 600 nm (OD_{600}) of 0.5. Cells were induced with 1.0 mM isopropyl-β-D-thiogalactopyranoside and grown for 68 h at 17°C. Cells were harvested by centrifugation at 3,730 × *g* for 15 min (JLA-10.500 rotor, 4°C) and resuspended in 80 ml 100 mM Tris-HCl (pH 8.0) supplemented with 10% (vol/vol) glycerol, 150 mM NaCl, and 10 μM FAD. The cell extract was obtained after cell disruption at 25,000 lb/in^2 (Constant Systems [Daventry, United Kingdom] cell disrupter) and subsequently centrifuged for 1 h at 29,100 × *g* (JA-17 rotor, 4°C). All subsequent steps were performed at 4°C. The soluble fraction was mixed with 2 ml preequilibrated Ni-Sepharose resin (GE-Healthcare) for 1.5 h. The flowthrough was removed, and the column was washed with 5 column volumes (CV) of 50 mM Tris-HCl with 150 mM NaCl and subsequently washed with 3 CV of 50 mM Tris-HCl with 150 mM NaCl containing 5 mM imidazole. The protein was eluted with 4 CV of 50 mM Tris-HCl with 150 mM NaCl containing 500 mM imidazole. The eluate was desalted on a Bio-Rad 10DG column.

To remove the N-terminal His_6-SUMO fusion from the HMFO protein, 4.3 mg purified SUMO-HMFO was cleaved with 0.2 mg SUMO-protease in 50 mM Tris-HCl (pH 8.0) in a total volume of 3.0 ml. The enzymes were incubated for 16 h at 4°C, and afterwards the solution was incubated with 0.4 ml preequilibrated Ni-Sepharose for 1.5 h at 4°C. HMFO was present in the flowthrough. The protease and the His-SUMO fragment were eluted with 50 mM Tris-HCl with 150 mM NaCl containing 500 mM imidazole. As a negative control, SUMO-HMFO was treated the same way as described above but no protease was added.

The UV-visual light spectrum of the purified protein was recorded between 240 and 650 nm. HMFO was denatured with a final concentration of 0.1% (wt/vol) SDS to obtain the spectrum of the free flavin cofactor. The spectra of folded and denatured HMFO were used to calculate both the concentration and the extinction coefficient of HMFO.

H467A mutation. To introduce the His467Ala mutation into HMFO, a whole-plasmid PCR was performed. For the H467A mutation, the following primers were used: forward, 5′-CGGCGGTGTTTGGGCTGCGAGCGGCACG-3′; reverse, 5′-CGTGCCGCTCGCAGCCCAAACACCGCCG-3′. Underlined bases are mismatches introducing Ala (GCT) instead of His (CAT). Template DNA was cleaved with DpnI (New England BioLabs). The plasmid was purified with a PCR purification kit (Qiagen) and transformed into *E. coli* TOP10 cells. The introduction of the mutations was confirmed by sequencing. Purification and spectral analysis of this mutant enzyme were performed as for the wild-type enzyme.

Temperature and pH optima of HMFO. To determine the temperature optimum of HMFO, 2.0 mM 4-hydroxybenzyl alcohol was oxidized in 50 mM phosphate buffer, pH 8.0. Observed rates were calculated on the basis of the increase in absorbance at 330 nm caused by the formation of 4-hydroxybenzaldehyde (ε_{330} = 13.7 $mM^{-1} \cdot cm^{-1}$ at 25°C). The cuvette containing the substrate dissolved in buffer was heated along with the spectrophotometer prior to the measurement, from 25 to 70°C. To start the measurement, 100 nM enzyme was added.

The pH optimum was determined with 100 nM HMFO and 2.0 mM 4-hydroxybenzyl alcohol in 12-fold-diluted Britton-Robinson buffer containing 200 mM boric acid, 200 mM acetic acid, and 200 mM phosphoric acid adjusted to the correct pH with NaOH. Activity was assayed from pH 6.5 to pH 10. Observed rates were calculated by using the formation of 4-hydroxybenzaldehyde as described above. The extinction coefficient of 4-hydroxybenzaldehyde was determined for all of the pH values measured.

ThermoFAD on HMFO variants. The unfolding temperatures of purified HMFO, SUMO-HMFO, and the SUMO-HMFO H467A mutant enzyme were analyzed by the ThermoFAD method (17). By this method, the release of the flavin cofactor is monitored while heating the enzyme. A real-time PCR thermocycler was used to denature 20 μl of 10 μM enzyme. The temperature gradient was set at 20 to 90°C, and fluorescence was measured every 0.5°C.

Activity measurements. The substrate range of HMFO was determined by using a peroxidase-coupled assay to detect H_2O_2 formed upon oxidation or by using a direct method that measures oxygen consumption upon the oxidation of the substrate. The alcohols assayed were 2-furanmethanol (furfuryl alcohol), HMF, (*S*)-5-hydroxymethyl-2(5H)-furanone, D-fructose, (1*R*,2*S*)-cyclohexane-1,2-diol, propane-1,2,3-triol (glycerol), (2*S*,4*R*)-pentan-1,2,3,4,5-pentol (D-xylitol), 2-hydroxy-*N*,*N*,*N*-trimethylethanaminium (choline), (2*E*,4*E*)-hexa-2,4-dien-1-ol, benzyl alcohol, 4-hydroxybenzylalcohol, 4-aminobenzyl alcohol, 4-chlorobenzyl alcohol, 4-(hydroxymethyl)-2-methoxyphenol (vanillyl alcohol), 2-methoxy-4-(2-propenyl)phenol, 1,3-dihydroxymethylbenzene, (*S*)-1-phenylethanol, (*R*)-1-phenylethanol, 2-phenylethanol, 4-butylbenzyl alcohol, (*S*)-phenyl-1,2-ethanediol, (*R*)-phenyl-1,2-ethanediol, 4,5-bis(hydroxylmethyl)-2-methylpyridin-3-ol (all purchased from Sigma), 5-hydroxymethyl-2-furfuryl alcohol (HMF-OH; TCI), (2E)-3-phenylprop-2-en-1-ol (cinnamyl alcohol; Acros), and 5-hydroxymethyl-2-furoic acid (HMF acid; Matrix Scientific). Because the latter was highly esterified, prior to use, 300 mM HMF acid was boiled in 2 M H_2SO_4 for 2 h. After hydrolysis, its pH was adjusted to 8.0 with NaOH and it was diluted to the proper concentration in 50 mM phosphate buffer (pH 8.0).

The aldehydes tested were 2-furancarboxaldehyde (furfural), DFF (both from Sigma), and 5-formyl-2-furancarboxylic acid (FFA; TRC). Also included in the screening were 1-phenyl-methylamine (Sigma) and 2-methoxy-4-(2-propenyl)phenol (Sigma).

In the coupled H_2O_2 detection assay, horseradish peroxidase (HRP [Sigma], 20 or 50 U/ml) oxidizes 4-aminoantipyrine (0.1 mM) and 3,5-dichloro-2-hydroxybenzenesulfonic acid (1 mM) to form a pink product that was measured at 515 nm (ε_{515} = 26 mM^{-1} cm^{-1}) (18). Oxygen concentrations were determined with REDFLASH sensor spots and a Firesting O_2 detector and light source (Pyroscience, Aachen, Germany). For calibration, a 100% oxygen solution was prepared by stirring MilliQ-water at 2,500 rpm for 15 min while exposed to air. This resulted in a 274 μM solution (23°C, pH 7.0, atmospheric pressure). The water was flushed with argon for 30 min to make the anoxic standard. The activity of 0.1 to 15 μM HMFO was assayed with 0.5 to 50 mM substrate, depending on the substrate used. All reactions were performed at 25°C in 50 mM phosphate buffer, pH 8.0.

The k_{cat} and K_m values for most of the substrates of SUMO-HMFO were determined by monitoring oxygen consumption during catalysis. A final concentration of 100 to 500 nM HMFO (depending on the substrate) was added to the substrate (0.01 to 100 mM) in 50 mM phosphate buffer (pH 8.0) at 25°C. The substrates used were furfuryl alcohol, furfural, HMF-OH, HMF, HMF acid, DFF, FFA, benzyl alcohol, 1,3-dihydroxymethylbenzene, 1,4-dihydroxymethylbenzene, 4-butylbenzyl alcohol, 4-hydroxybenzyl alcohol, 4-aminobenzyl alcohol, 4-chlorobenzyl alcohol, cinnamyl alcohol, and (2*E*,4*E*)-hexa-2,4-dien-1-ol. Oxygen concentrations were determined with REDFLASH sensor spots as mentioned above. The rates of oxygen decrease were converted to observed rates, and the Michaelis-Menten kinetic parameters were obtained by curve fitting with the formula $v = (k_{cat} \cdot [S])/(K_m + [S])$ and SigmaPlot. The k_{cat} and K_m values of both the wild-type and H467A mutant enzymes for vanillyl alcohol were determined. Product formation was monitored spectrophotometrically by measuring the increase in absorption at 340 nm (ε_{340} = 14 mM^{-1} cm^{-1}). The substrate concentrations used were as described above. For the wild-type enzyme, 200 nM enzyme was used, while for the H467A mutant enzyme, 5.0 μM was used. The oxidase activity of the wild-type enzyme (5.0 μM) on glycerol was monitored with the coupled HRP assay described above. Initial rates were measured on glycerol at concentrations ranging from 1.0 mM to 1.0 M.

Formation of H_2O_2. The production of H_2O_2 as a by-product of catalysis was detected with catalase (Sigma). For this, 100 μM cinnamyl alcohol was oxidized with 0.2 μM HMFO. When the oxygen level no longer decreased, 150 U of catalase was added to monitor the reappearance of oxygen. Oxygen levels were monitored with REDFLASH sensor spots and a Firesting O_2 detector and light source (Pyroscience, Aachen, Germany).

Product identification. The products formed by HMFO with HMF as the substrate were analyzed with a Zorbax Eclipse XDB-C8 column (5 μm; Agilent). As the mobile phase, 12 mM phosphate buffer at pH 7.0 (A) and acetonitrile (B) were used at a flow rate of 1.2 ml min^{-1}. After 1 min of 100% A, B was increased to 5% in 3.5 min and subsequently to 40% in 2.5 min. After 0.5 min of 40% B, the eluent was returned to 100% A in 0.5 min and this level was maintained for 2 min. Detection was done at 268 nm. The retention times of HMF, DFF, HMF acid, FFA, and FDCA were 6.4, 6.0, 1.6, 2.1, and 1.2 min, respectively. Calibration curves were made with 0.1, 0.5, 1.0, and 2.0 mM solutions.

Product formation was analyzed after 5 h of conversion of 2 mM HMF by 5 μM HMFO (25°C, 600 rpm). The reaction mixtures were heated at 80°C for 5 min to inactivate the enzyme, and protein aggregates were subsequently removed by centrifugation. As negative controls, solutions of HMF, DFF, HMF acid, and FFA were treated in the same way but in the absence of enzyme to monitor the spontaneous oxidation of the substrate and the intermediates by air.

RESULTS

Identification and cloning of the HMFO-encoding gene. For a more detailed study of the HMF-oxidizing enzyme of *C. basilensis*, we first tried to express HmfH in *E. coli*. For this, several pBAD- and pET-based expression plasmids were used while testing a variety of *E. coli* strains, growth temperatures, and inducer concentrations. In addition to the native *hmfH* gene, several expression-optimized genes were included in the expression tests. However, no soluble expression of HmfH could be achieved, even when using maltose binding protein or SUMO as a fusion partner to boost the expression of soluble protein (results not shown). Therefore, we decided to look for homologous genes for which the corresponding enzymes are expected to fulfill a similar metabolic role. A sequence database BLAST search revealed several homologues of HmfH, all with unknown functions. The closest homologues are mainly from *Burkholderia* species (32 to 69% sequence identity), while genes from other bacteria were also identified. We decided to continue with two homologous genes, one from *B. phytofirmans* PsJN (YP_001895804.1) and one from *Methylovorus* sp. strain MP688 (YP_004038556.1). The encoded proteins showed 69 and 46% sequence identity with the HmfH protein sequence (see Fig. S4 in the supplemental material). The genes that encode these homologues were ordered as expression-optimized genes in a pJexpress 404 vector. Like HmfH, the protein from *B. phytofirmans* PsJN could not be expressed in *E. coli*. The *Methylovorus* homologue could be functionally expressed. Because expression was limited with this construct, a pET-SUMO fusion construct was generated, resulting in a 20-fold increase in expression.

Structural and spectral properties of HMFO. From 1 liter of a culture with an OD_{600} of 20, it was possible to purify 88 mg of yellow SUMO-HMFO. The purified protein runs as a single band with a mass of around 70 kDa on SDS-PAGE. This is in agreement with the 70.4-kDa predicted mass of the His_6-SUMO-HMFO fusion protein. When the SDS-PAGE gel was soaked in 5% acetic acid, no UV fluorescent band could be detected, suggesting that the flavin cofactor is not covalently bound to the protein. A close

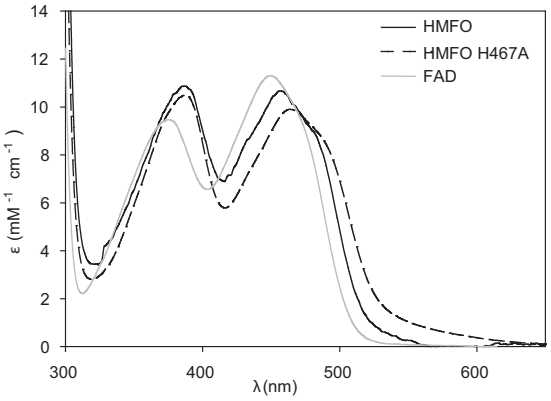

FIG 2 Absorption spectra of recombinant wild-type HMFO, SUMO-HMFO H467A, and FAD.

homologue with a known structure is choline oxidase (EC 1.1.3.17; CholO) from *Arthrobacter globiformis* (32% sequence identity). In this protein, the FAD cofactor is covalently linked via an 8-α-histidyl bond. A pairwise sequence alignment shows that the respective histidine responsible for the protein-FAD bond, His99, is not conserved in HMFO (Val101 in this position). To verify that the flavin cofactor is dissociable, HMFO was subjected to trichloroacetic acid treatment and subsequent centrifugation. This indeed resulted in the formation of a white protein pellet and a yellow supernatant.

The UV-visual light spectrum of the native enzyme was a typical flavoprotein absorbance spectrum with absorbance maxima at 385 and 456 nm. Upon unfolding by SDS, a flavin spectrum was obtained that was identical to that of commercially available FAD, with an absorbance maximum at 450 nm. Using the known extinction constant for FAD (ε_{450} = 11.3 mM^{-1} cm^{-1}), the extinction constant for HMFO (ε_{456} = 10.7 mM^{-1} cm^{-1}) could be determined (Fig. 2).

To probe whether the SUMO fusion tag has an effect on the properties of HMFO, the N-terminal SUMO part was cleaved off by proteolytic treatment of the fusion enzyme with SUMO protease. The recombinant wild-type HMFO generated was compared with the fused variant by measuring their UV-visual spectra, determining their steady-state kinetic parameters for HMF, and measuring their thermostability. These results show that neither the flavin spectrum (indicative of an identical microenvironment around the flavin cofactor), nor the activity of HMFO (differences between K_m and k_{cat} values, <10%), nor its thermostability (apparent melting temperatures differed <0.5°C) was affected by fusing it to SUMO at the N terminus. Therefore, we decided to use SUMO-fused HMFO for the rest of our study.

Substrate specificity of HMFO. HMFO was identified with a BLASTp search as a homologue (46% sequence identity) of HmfH of *C. basilensis*. The latter protein is thought to be active on HMF. Hence, purified HMFO was assayed for activity with HMF. An enzyme-dependent decrease in molecular oxygen showed that HMFO is active on HMF. This matches the prediction that HMFO is a member of the GMC-type oxidase family. In most oxidases, molecular oxygen is used to reoxidize the flavin cofactor, resulting in the formation of H_2O_2. For HMFO, hydrogen peroxide formation was experimentally confirmed by adding catalase after the incubation of HMFO and cinnamyl alcohol. During catalysis, 0.08 mM molecular oxygen was consumed. The addition of 150 U of catalase resulted in the formation of 0.04 mM molecular oxygen, showing that HMFO is an oxidase.

Enzymatic oxidation of HMF is of interest for the production of FDCA. As shown in Fig. 1, this conversion consists of three oxidation steps. Therefore, the activity of HMFO on the intermediates DFF, HMF acid, and FFA was also measured. Surprisingly, HMFO was also found to convert DFF and HMF acid. Although chemically related, all of these furans have different properties. This is clearly reflected in the k_{cat} and K_m values obtained (Table 1). The affinity of HMFO for HMF is 50-fold higher than that for HMF acid, possibly because of the negative charge introduced by the carboxylic acid. Intriguing is the activity of HMFO on DFF, an aldehyde. Oxidation of aldehydes is not a common feature of GMC-type oxidases. Several alcohol-aldehyde couples were analyzed. For DFF, the k_{cat}/K_m value for DFF is only seven times lower than that for the analogous alcohol HMF-OH. A similar alcohol-aldehyde couple is furfuryl alcohol and furfural. The kinetic parameters for furfuryl alcohol are comparable to those for HMF-OH. Furfural, on the other hand, is not a substrate.

We discovered that the substrate acceptance profile of HMFO is not restricted to furans. Benzylic alcohols are readily accepted by the enzyme too. In fact, HMFO is active on all of the primary alcohols tested (both furan and benzyl). The k_{cat} values on all of these alcohols are rather similar (Table 1).

Like other GMC oxidoreductases, HMFO seems to be restricted to carbon oxygen bond oxidation. For instance, the amine benzylamine is not a substrate whereas benzyl alcohol is. In addition, hydroxylation of a double bond, as performed by the FAD-containing vanillyl alcohol oxidase (19), cannot be performed by HMFO.

Product identification. To establish the identity of HMFO-formed products, high-performance liquid chromatography analysis was performed. After 5 h of incubation, 2 mM HMF was fully converted by 5 μM HMFO (Fig. 3). The main product of the reaction was FFA (92%), but a considerable amount of FDCA (8%) was also present. In a control reaction mixture without HMFO, HMF remained the main component (>99%), which implies that HMFO is needed for the conversion of HMF. To exclude the spontaneous oxidation of the intermediates (HMF acid, DFF, and FFA) in time, similar control reaction mixtures were prepared with these HMF derivatives. In all cases, >99% of the HMF derivatives detected were the starting compounds. This excludes the spontaneous formation of FDCA and confirms that HMFO can produce FDCA.

Temperature and pH optima of HMFO. To establish the optimal conditions for HMFO, its pH and temperature optima were determined. Activity was determined between pH 6.5 and pH 10 in Britton-Robinson buffer. The optimal pH of HMFO for activity was 8.0, and it retained almost 80% of its peak activity between pH 6.5 and pH 9.0. At pH 10.0, its activity decreased to 30% (Fig. 4A). The Britton-Robinson buffer used reduced the activity of HMFO by 10% compared to that obtained with phosphate buffer at pH 8.0.

The temperature optimum was determined between 25 and 70°C. HMFO was most active at 55°C. At 25°C, HMFO had 60% of the activity that it had at 55°C, and at 70°C, only 10% of its activity was left (Fig. 4B). By using the ThermoFAD method, we determined that its apparent melting temperature was 48.5°C. This shows that the oxidase is reasonably thermotolerant.

TABLE 1 Steady-state kinetic parameters of HMFO[a]

Substrate	Structure	k_{cat} (s^{-1})	K_m (mM)	k_{cat}/K_m ($s^{-1}\,M^{-1}$)
Furfuryl alcohol	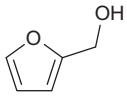	11.9	7.9	1,500
Furfural	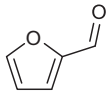	ND[d]	ND	<10
HMF-OH	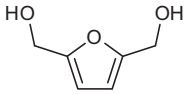	21.5	5.7	3,900
HMF	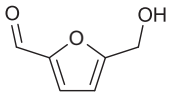	9.9	1.4	7,100
DFF	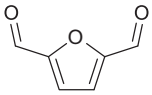	1.6	1.7	940
HMF acid	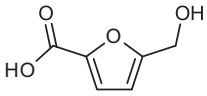	8.5	73	120
FFA	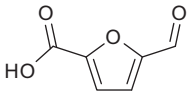	ND	ND	<10
1,4-Benzenedimethanol	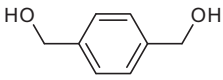	21.1	1.4	15,000
1,3-Benzenedimethanol		14.0	1.5	9,300
Benzyl alcohol	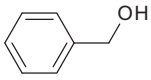	13.5	1.3	10,000
4-Hydroxybenzyl alcohol	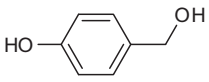	7.2	0.3	24,000
4-Aminobenzyl alcohol	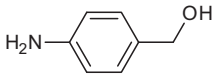	17.1	1.44	12,000
4-Chlorobenzyl alcohol	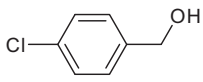	9.5	0.08	120,000
4-Butylbenzyl alcohol	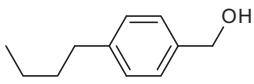	10.0	2.8	3,600

(Continued on following page)

TABLE 1 (Continued)

Substrate	Structure	k_{cat} (s^{-1})	K_m (mM)	k_{cat}/K_m ($s^{-1}\,M^{-1}$)
1-Phenylethanol	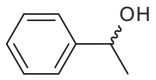	ND	ND	ND
Cinnamyl alcohol	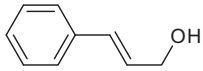	17.0	0.07	260,000
2,4-Hexadien-1-ol	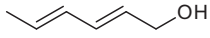	13.3	0.59	23,000
Glycerol[b]	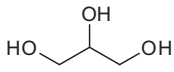	ND	ND	<1
Vanillyl alcohol[c]	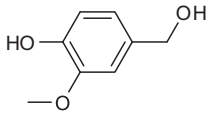	21.0	0.73	29,000
HMFO H467A: vanillyl alcohol[c]	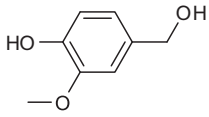	$4.7{\cdot}10^{-3}$	0.82	5.7

[a] The kinetic parameters of HMFO are determined in a 50 mM potassium phosphate buffer (pH 8.0) at 25°C with REDFLASH sensor spots and a Firesting O_2 detector and light source on all substrates unless stated otherwise.
[b] Kinetic parameters were determined by H_2O_2 formation in a coupled assay.
[c] Kinetic parameters were calculated from the increase in the product's absorbance at 340 nm.
[d] ND, not determined.

Identification of an active-site histidine, H467. One key feature of GMC-type oxidases is the presence of an absolutely conserved histidine in the C-terminal domain. The role of this histidine has been investigated in well-studied GMC family members such as glucose oxidase, choline oxidase (CholO), and aryl alcohol oxidase (AAO) (13, 20, 21). Replacement of this histidine with alanine resulted in a drastic reduction of the catalysis of all of these oxidases. A homology model of HMFO was made by using the crystal structures of pyranose oxidase (3T37) and CholO (3NNE). Inspection of this model revealed H467 as the active-site histidine in HMFO. As expected, catalysis of HMFO H467A is severely reduced compared to that of the wild-type enzyme. With vanillyl alcohol as the substrate, the k_{cat} value of the mutant enzyme is 4,400 times lower than that of the wild-type enzyme. The affinity for the substrate is, however, hardly affected (Table 1). The microenvironment of the flavin is also altered in the mutant enzyme, as shown by the UV-visual light spectrum (Fig. 2). The absorbance maximum has shifted from 456 to 464 nm (ε_{464} = 9.9 $mM^{-1}\,cm^{-1}$). It is clear that the histidine does not play an important role in substrate binding, while it is essential for catalysis. Whether H467 is involved in the oxidative or reductive half reaction remains to be determined for HMFO.

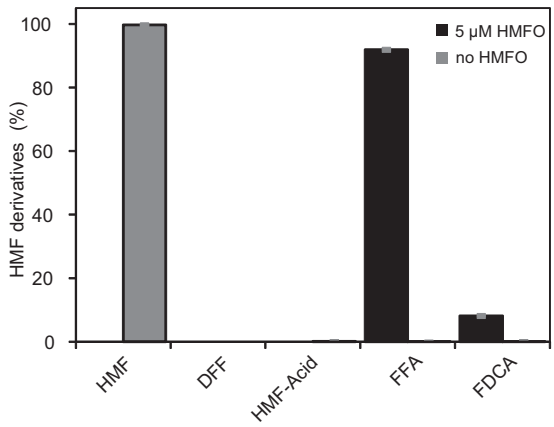

FIG 3 Product formation by HMFO. The black bars represent the products formed by 5 μM HMFO starting with 2 mM HMF as the substrate. HMF is fully converted into FFA (92%) and FDCA (8%). In a control experiment without the enzyme (gray bars), HMF remained present. Less than 0.5% HMF acid and FFA were present. All experiment were performed in duplicate, and average values are shown with standard deviation displayed as gray bars.

DISCUSSION

HMFO was identified as a homologue of HmfH from *C. basilensis* (8). The latter protein is thought to be active on HMF. Although it is only 45% identical to HmfH and lacks a 35-amino-acid-long part near the C terminus of the protein, HMFO is active on HMF as well. The substrate profile of HMFO is, however, not restricted to HMF. Many other furans and also benzylic compounds are accepted by the enzyme. Among the substrates tested, the enzyme shows activity on all aromatic compounds with a methanol

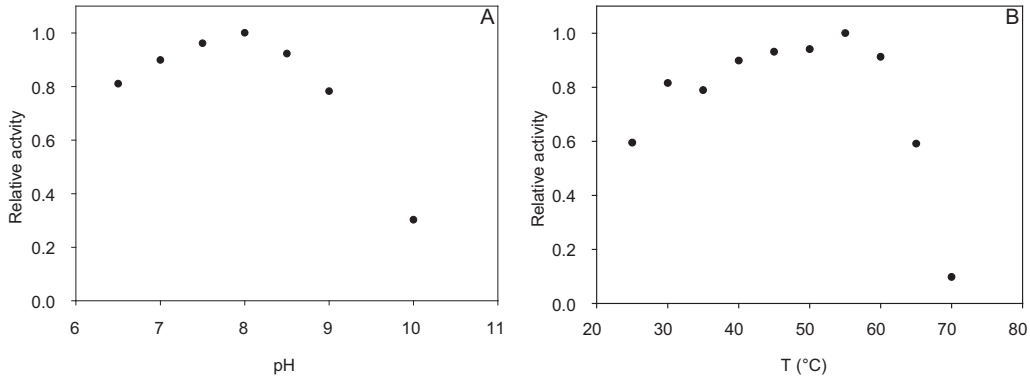

FIG 4 (A) Optimum pH for HMFO activity. The activity of HMFO on 4-hydroxybenzyl alcohol as measured in Britton-Robinson buffer is shown. (B) Optimum temperature (T) for HMFO activity based on the activity of HMFO on 4-hydroxybenzyl alcohol between 25 and 70°C. The maximal activity at 55°C was assigned a value of 1.

substituent. This shows that, in addition to aromaticity, the position and nature of the alcohol are important. This strict specificity for primary alcohols is likely due to the specific architecture of the active site. The best-supported reaction mechanism for GMC oxidases involves the abstraction of a proton from the alcohol group as the initial step of catalysis (22). If the substituent is more bulky, the alcohol moiety may not be positioned close enough to facilitate hydride transfer to the flavin cofactor. Alternatively, deprotonation of the alcohol by the active-site base is obstructed.

Another requirement is the presence of a conjugated system within the molecule, illustrated by, for instance, cinnamyl alcohol and 2,4-hexadien-1-ol. The planar structure caused by the double-bond system might be a requirement for productive binding of the substrate. Alternatively, the conjugated system is extended when the alcohol is oxidized to the aldehyde and might thereby facilitate alcohol oxidation.

Because the enzyme is not active on secondary alcohols, we could not demonstrate enantiospecificity for this oxidase. This does not mean that the enzyme is not stereospecific; it will most likely abstract a hydride in a preferred stereospecific manner. The C-α atom of the alcohol moiety contains two hydrogens, of which one will be selectively abstracted. For *Pleurotus eryngii* AAO (23), it has been shown by using monodeteurated *p*-methoxybenzyl alcohol that the enzyme abstracts only the R hydrogen, which is closest to the flavin N5, as a hydride. Future structural and kinetic studies will reveal whether HMFO acts via a similar mechanism.

The rates of catalysis on all identified substrates are fairly similar, regardless of the substituents on the aromatic ring. With the *para*-substituted, electron-donating groups of 4-aminobenzyl alcohol and 4-hydroxybenzyl alcohol, k_{cat} values similar to those obtained with an electron-withdrawing halide, as in 4-chlorobenzyl alcohol, were obtained. All of these rates are comparable to those obtained with the nonsubstituted benzyl alcohol. The ring substituents are, however, of great importance for the affinity of HMFO for its substrate. The negatively charged carboxylic acid of HMF acid reduces its affinity >10-fold compared to that for most nonsubstituted substrates. 4-Chlorobenzyl alcohol, on the other hand, has a 16-fold lower K_m value than the nonsubstituted benzyl alcohol.

The relaxed substrate profile of HMFO makes it an interesting biocatalyst for the oxidation of aromatic alcohols. Moreover, HMFO not only oxidizes a wide variety of aromatic alcohols, it can also perform aldehyde oxidations. Aldehyde oxidation is not a general feature of GMC oxidases. A notable exception is choline oxidase (EC 1.1.3.17) (24), but for fungal AAOs (EC 1.1.3.7), aldehyde oxidation has been demonstrated as well (15, 25). For these GMC oxidases, it was shown that the hydrated aldehyde, the *gem*-diol, is the actual substrate. As a consequence, the reactivity of aldehydes as substrates is greatly affected by the nature of the substituents on the aromatic ring. Electron-withdrawing groups, like carbonyl substituents, both deactivate and activate the aldehyde. Hydride transfer is hampered because electrons are withdrawn from the aldehyde. On the other hand, the aldehyde is more easily hydrated when an electron-withdrawing group is present. Having more substrate in the hydrated form could therefore lead to faster oxidation (25). Because of the deactivating and activating effects of a single substituent, it is hard to predict which effect a substituent will have on catalysis.

For the full oxidation of HMF to form FDCA, both alcohol and aldehyde groups have to be oxidized. Product analysis revealed that FDCA is formed by HMFO. FFA was the only intermediate observed, whereas the single oxidized intermediates (HMF acid and DFF) where not detected (Fig. 3). This illustrates the effect of the activating or deactivating groups on aldehyde oxidation, as described above. In FFA, the carboxylic acid in the 2 position might hamper the oxidation of the aldehyde in the 5 position. However, when the furan ring contains an aldehyde substituent (DFF) instead of a carboxylic acid, the reactivity increases (Table 1). The formation of FFA as the main product is in agreement with the rates listed in Table 1, as it is the only intermediate between HMF and FDCA on which catalysis was poor.

The substrate profile and the ability to oxidize aromatic alcohols and aldehydes reveal a striking resemblance between HMFO and the fungal AAOs. Both enzyme types belong to the same flavoprotein oxidase family. However, the sequence similarity between these oxidases is not indicative of a strong functional relationship (sequence identity, <30%). The physiological roles of the two oxidase types are also clearly different. AAOs are secreted by fungi to assist in the degradation of lignin, while the bacterial HMFO is an intracellular enzyme. This prohibits a direct role in lignin degradation. In view of the sequence similarity of the HMFO-encoding gene to the *hmfH* gene of *C. basilensis*, which is involved in HMF degradation, it is tempting to conclude that also

HMFO is part of an HMF degradation pathway. The typical gene cluster found in HMF-degrading bacteria (26) is, however, not present in *Methylovorus* sp. strain MP688.

To identify catalytically important residues in HMFO, a homology model of HMFO was prepared by using the YASARA software (27). The best-studied close homologue of HMFO with a known crystal structure is CholO. Comparison of the HMFO model structure with the structure of CholO reveals that several catalytically important residues of CholO are not conserved. The negatively charged Glu312 residue of CholO, for instance, positions the positively charged amine of choline and is therefore not conserved because the substrates of HMFO do not contain a positive charge. In addition, choline is not a substrate for HMFO. Other catalytically important residues, like His307, Val465, and His467 (His310, Val464, and His466 in CholO), are conserved. For CholO, it has been shown that mutation of active-site histidine His466 to alanine decreases the reaction rate 60-fold and increases the Michaelis constant 17-fold (20). In our study, the analogous mutation was introduced into HMFO. This resulted in a 4,400-fold decrease in the k_{cat} value, whereas the K_m value was hardly affected, confirming the importance of this residue for catalysis. In studies on AAO from *P. eryngii*, His502 was replaced with alanine, resulting in a decrease in the k_{cat} value of almost 3,000-fold, similar to the effect seen in the HMFO mutant enzyme. The mutation also increased the K_m value 80-fold, an effect much more severe than that observed in HMFO (21). Studies on CholO and AAO from *P. eryngii* suggest that this histidine is the active-site base (28). The role of His467 in HMFO is likely to be similar.

The identification and characterization of an HMF-oxidizing oxidase adds a new tool with which to develop a biocatalytic process for the production of FDCA from HMF. HMFO is the first characterized enzyme able to oxidize HMF and produce FDCA. In addition, the enzyme can perform selective oxidations on many benzylic substrates. The substrate profile resembles the substrate acceptance of fungal AAOs to a large extent. The production of these fungal oxidases in a recombinant form has been shown to be difficult. Therefore, HMFO may also develop as a biocatalytic alternative for these oxidases. Overall, HMFO is a suitable catalyst for applications involving selective alcohol and aldehyde oxidations.

ACKNOWLEDGMENT

This work was carried out within the BE-Basic R&D Program, for which an FES subsidy was granted from the Dutch Ministry of Economic Affairs, Agriculture, and Innovation (EL&I).

REFERENCES

1. **Kamm B.** 2007. Production of platform chemicals and synthesis gas from biomass. Angew. Chem. Int. Ed. Engl. **46:**5056–5058. doi:http://dx.doi.org/10.1002/anie.200604514.
2. **Moreau C, Naceur M, Gandini A.** 2004. Recent catalytic advances in the chemistry of substituted furans from carbohydrates and in the ensuing polymers. Top. Catal. **27:**11–30. http://dx.doi.org/10.1023/B:TOCA.0000013537.13540.0e.
3. **van Putten R-J, Soetedjo JNM, Pidko EA, van der Waal JC, Hensen EJM, de Jong E, Heeres HJ.** 2013. Dehydration of different ketoses and aldoses to 5-hydroxymethylfurfural. ChemSusChem **6:**1681–1687. http://dx.doi.org/10.1002/cssc.201300345.
4. **Carlini C, Patrono P, Galletti AMR, Sbrana G, Zima V.** 2005. Selective oxidation of 5-hydroxymethyl-2-furaldehyde to furan-2,5-dicarboxaldehyde by catalytic systems based on vanadyl phosphate. Appl. Catal. A Gen. **289:**197–204. http://dx.doi.org/10.1016/j.apcata.2005.05.006.
5. **Casanova O, Iborra S, Corma A.** 2009. Biomass into chemicals: aerobic oxidation of 5-hydroxymethyl-2-furfural into 2,5-furandicarboxylic acid with gold nanoparticle catalysts. ChemSusChem **2:**1138–1144. http://dx.doi.org/10.1002/cssc.200900137.
6. **Laadan B, Almeida RM, Peter R.** 2008. Identification of an NADH-dependent 5-hydroxymethylfurfural-reducing alcohol dehydrogenase in *Saccharomyces cerevisiae*. Yeast **25:**191–198. http://dx.doi.org/10.1002/yea.1578.
7. **van Deurzen MPJ, van Rantwijk F, Sheldon RA.** 1997. Chloroperoxidase-catalyzed oxidation of 5-hydroxy methylfurfural. J. Carbohydr. Chem. **16:**299–309.
8. **Wierckx N, Koopman F, Bandounas L, de Winde JH, Ruijssenaars HJ.** 2010. Isolation and characterization of *Cupriavidus basilensis* HMF14 for biological removal of inhibitors from lignocellulosic hydrolysate. Microb. Biotechnol. **3:**336–343. http://dx.doi.org/10.1111/j.1751-7915.2009.00158.x.
9. **Koopman F, Wierckx N, de Winde JH, Ruijssenaars HJ.** 2010. Efficient whole-cell biotransformation of 5-(hydroxymethyl)furfural into FDCA, 2,5-furandicarboxylic acid. Bioresour. Technol. **101:**6291–6296. http://dx.doi.org/10.1016/j.biortech.2010.03.050.
10. **Dijkman WP, Gonzalo G, Mattevi A, Fraaije MW.** 2013. Flavoprotein oxidases: classification and applications. Appl. Microbiol. Biotechnol. **97:**5177–5188. http://dx.doi.org/10.1007/s00253-013-4925-7.
11. **Bannwarth M, Bastian S, Heckmann-Pohl D, Giffhorn F, Schulz GE.** 2004. Crystal structure of pyranose 2-oxidase from the white-rot fungus *Peniophora* sp. Biochemistry **43:**11683–11690. http://dx.doi.org/10.1021/bi048609q.
12. **Ikuta S, Imamura S, Misaki H, Horiuti Y.** 1977. Purification and characterization of choline oxidase from *Arthrobacter globiformis*. J. Biochem. **82:**1741–1749.
13. **Roth JP, Klinman JP.** 2003. Catalysis of electron transfer during activation of O_2 by the flavoprotein glucose oxidase. Proc. Natl. Acad. Sci. U. S. A. **100:**62–67. http://dx.doi.org/10.1073/pnas.252644599.
14. **Kaneda Y, Ohnishi K, Yagi T.** 2002. Purification, molecular cloning, and characterization of pyridoxine 4-oxidase from *Microbacterium luteolum*. Biosci. Biotechnol. Biochem. **66:**1022–1031. http://dx.doi.org/10.1271/bbb.66.1022.
15. **Romero E, Ferreira P, Martínez AT, Martínez MJ.** 2009. New oxidase from *Bjerkandera* arthroconidial anamorph that oxidizes both phenolic and nonphenolic benzyl alcohols. Biochim. Biophys. Acta **1794:**689–697. http://dx.doi.org/10.1016/j.bbapap.2008.11.013.
16. **Jin J, Mazon H, van den Heuvel RHH, Janssen DB, Fraaije MW.** 2007. Discovery of a eugenol oxidase from *Rhodococcus* sp. strain RHA1. FEBS J. **274:**2311–2321. http://dx.doi.org/10.1111/j.1742-4658.2007.05767.x.
17. **Forneris F, Orru R, Bonivento D, Chiarelli LR, Mattevi A.** 2009. ThermoFAD, a thermofluor-adapted flavin ad hoc detection system for protein folding and ligand binding. FEBS J. **276:**2833–2840. http://dx.doi.org/10.1111/j.1742-4658.2009.07006.x.
18. **Heuts DPHM, van Hellemond EW, Janssen DB, Fraaije MW.** 2007. Discovery, characterization, and kinetic analysis of an alditol oxidase from *Streptomyces coelicolor*. J. Biol. Chem. **282:**20283–20291. http://dx.doi.org/10.1074/jbc.M610849200.
19. **Fraaije MW, Veeger C, van Berkel WJ.** 1995. Substrate specificity of flavin-dependent vanillyl-alcohol oxidase from *Penicillium simplicissimum*. Evidence for the production of 4-hydroxycinnamyl alcohols from 4-allylphenols. Eur. J. Biochem. **234:**271–277.
20. **Ghanem M, Gadda G.** 2005. On the catalytic role of the conserved active site residue His466 of choline oxidase. Biochemistry **44:**893–904. http://dx.doi.org/10.1021/bi048056j.
21. **Hernández-Ortega A, Lucas F, Ferreira P, Medina M, Guallar V, Martínez AT.** 2012. Role of active site histidines in the two half-reactions of the aryl-alcohol oxidase catalytic cycle. Biochemistry **51:**6595–6608. http://dx.doi.org/10.1021/bi300505z.
22. **Gadda G.** 2008. Hydride transfer made easy in the reaction of alcohol oxidation catalyzed by flavin-dependent oxidases. Biochemistry **47:**13745–13753. http://dx.doi.org/10.1021/bi801994c.
23. **Hernández-Ortega A, Ferreira P, Merino P, Medina M, Guallar V, Martínez AT.** 2012. Stereoselective hydride transfer by aryl-alcohol oxidase, a member of the GMC superfamily. Chembiochem **13:**427–435. http://dx.doi.org/10.1002/cbic.201100709.
24. **Fan F, Ghanem M, Gadda G.** 2004. Cloning, sequence analysis, and purification of choline oxidase from *Arthrobacter globiformis*: a bacterial enzyme involved in osmotic stress tolerance. Arch. Biochem. Biophys. **421:**149–158. http://dx.doi.org/10.1016/j.abb.2003.10.003.

25. **Ferreira P, Hernández-Ortega A, Herguedas B, Rencoret J, Gutiérrez A, Martínez MJ, Jiménez-Barbero J, Medina M, Martínez AT.** 2010. Kinetic and chemical characterization of aldehyde oxidation by fungal aryl-alcohol oxidase. Biochem. J. **425:**585–593. http://dx.doi.org/10.1042/BJ20091499.
26. **Koopman F, Wierckx N, de Winde JH, Ruijssenaars HJ.** 2010. Identification and characterization of the furfural and 5-(hydroxymethyl)furfural degradation pathways of *Cupriavidus basilensis* HMF14. Proc. Natl. Acad. Sci. U. S. A. **107:**4919–4924. http://dx.doi.org/10.1073/pnas.0913039107.
27. **Krieger E, Koraimann G, Vriend G.** 2002. Increasing the precision of comparative models with YASARA NOVA—a self-parameterizing force field. Proteins Struct. Funct. Genet. **47:**393–402. http://dx.doi.org/10.1002/prot.10104.
28. **Hernández-Ortega A, Borrelli K, Ferreira P, Medina M, Martínez AT, Guallar V.** 2011. Substrate diffusion and oxidation in GMC oxidoreductases: an experimental and computational study on fungal aryl-alcohol oxidase. Biochem. J. **436:**341–350. http://dx.doi.org/10.1042/BJ20102090.